








Article

Glycerol Oxidation over Supported Gold Catalysts: The Combined Effect of Au Particle Size and Basicity of Support

Ekaterina Pakrieva ^{1,2}, Ekaterina Kolobova ¹, Dmitrii German ¹, Marta Stucchi ³, Alberto Villa ³, Laura Prati ³, Sónia. A.C. Carabineiro ⁴, Nina Bogdanchikova ⁵, Vicente Cortés Corberán ² and Alexey Pestryakov ^{1,*}

¹ Research School of Chemistry & Applied Biomedical Sciences, National Research Tomsk Polytechnic University, Lenin Av. 30, 634050 Tomsk, Russia; epakrieva@mail.ru (E.P.); ekaterina_kolobova@mail.ru (E.K.); germandmitry93@gmail.com (D.G.)

² Instituto de Catálisis y Petroleoquímica, Consejo Superior de Investigaciones Científicas, Marie Curie 2, 28049 Madrid, Spain; vcortes@icp.csic.es

³ Dipartimento di Chimica, Università degli Studi di Milano, via Golgi 19, 20133 Milano, Italy; marta.stucchi@unimi.it (M.S.); Alberto.Villa@unimi.it (A.V.); laura.prati@unimi.it (L.P.)

⁴ LAQV-REQUIMTE, Department of Chemistry, NOVA School of Science and Technology, Universidade NOVA de Lisboa, 2829-516 Caparica, Portugal; sonia.carabineiro@fct.unl.pt

⁵ Centro de Nanociencias y Nanotecnología, Universidad Nacional Autónoma de México, 22800 Ensenada, Mexico; nina@cnyn.unam.mx

* Correspondence: pestryakov2005@yandex.ru

Received: 29 July 2020; Accepted: 17 August 2020; Published: 20 August 2020



Abstract: Gold nanoparticles supported on various oxides (CeO₂, CeO₂/TiO₂, MgO, MgO/TiO₂, La₂O₃, La₂O₃/TiO₂) (with 4 wt.% Au loading) were investigated in the liquid (aqueous) phase oxidation of glycerol by molecular oxygen under mild conditions, in the presence of alkaline earth (CaO, SrO and MgO) or alkaline (NaOH) bases. Full conversion and selectivity between 38 and 68% to sodium glycerate were observed on different Au supported catalysts (Au/MgO/TiO₂, Au/La₂O₃/TiO₂, Au/CeO₂ and Au/CeO₂/TiO₂). The combined effect of Au particle size and basicity of the support was suggested as the determining factor of the activity. Agglomeration of gold nanoparticles, found after the reaction, led to the deactivation of the catalysts, which prevents the further oxidation of sodium glycerate into sodium tartronate. Promising results were obtained with the use of alkaline earth bases (CaO, SrO, MgO), leading to the formation of free carboxylic acids instead of salts, which are formed in the presence of the more usual base, NaOH.

Keywords: gold catalysts; glycerol oxidation; catalyst selectivity; glyceric acid; glycolic acid; tartronic acid; base additives

1. Introduction

Glycerol, a highly functionalized molecule, was identified as one of the top twelve most important bio-based chemicals in the world by the US Department of Energy [1]. Glycerol has a wide range of applications, from the production of food additives to pharmaceuticals, cosmetics, personal care products and detergents, and it is also transformed into non-toxic solvents [2–5].

Nowadays, glycerol is mostly generated as an undesired byproduct (around 10% of the total volume) during the production of biodiesel, one of the most important and valuable alternative liquid biofuels in the transportation sector [6–8]. In 2017, the production of biodiesel exceeded 21 million tons per year just in the EU [9]. Thus, despite the wide market for glycerol, the increasing growth

of the biodiesel industry leads to the problem how to utilize the glycerol glut. Moreover, the use of low-quality glycerol from biodiesel production involves complex and expensive purification processes. Therefore, adding value to glycerol could contribute to the commercial viability of biodiesel production.

Among the processes used to transform glycerol (oxidation/reduction, reaction with other molecules), selective oxidation by low-cost and environmentally-friendly heterogeneous catalytic methods allows glycerol to be converted into more valuable products. Using glycerol as a raw material can result in a range of useful oxygenated compounds, such as glyceric, tartronic, glycolic, lactic and hydroxypyruvic acids, and dihydroxyacetone. Hence, control of the product selectivity is crucial.

Selective oxidation of glycerol with molecular oxygen on supported precious metal catalysts, (Pd, Pt and notably Au) shows very high activity in the process [10–14]. Furthermore, compared with catalysts based on metals of the platinum group, gold catalysts appear to be more resistant to oxygen poisoning under liquid-phase oxidation conditions using O₂ as the oxidant [15]. However, to obtain significant glycerol conversion, the presence of an alkaline medium is necessary, because it contributes to the first step of the oxidation process, the deprotonation of glycerol, which is considered essential for the oxidation of primary alcohols [16]. A gold catalyst alone cannot activate the hydroxyl group of glycerol at mild temperatures [17].

The major oxidation products of glycerol obtained over gold-based catalysts in the presence of added bases are glyceric and glycolic acids and in some cases tartronic acid (Table 1, Scheme 1), which are produced by the sequential oxidation of glyceric acid. All these substances are valuable substrates for the chemical and pharmaceutical industry. Glyceric acid, is generally considered as the primary product from glycerol oxidation and is used in cosmetology as a carotolytic and as a base material for functional surfactants and monomer for oligoesters [18]. However, semi-industrial methods for the production of glyceric acid have not been developed yet, even though the general approaches of enzymatic synthesis [19,20] and the traditional methods for producing α -hydroxy acids by acid hydrolysis of cyanohydrins are still applicable. Glycolic acid is used in the textile industry as a dyeing and tanning agent, in food processing as a flavoring agent and as a preservative, and in the pharmaceutical industry as a skin care agent [21]. It is also used together with lactic acid, another high value glycerol oxidation product, to produce a co-polymer (poly (lactic-co-glycolic acid), PLGA) for medical application in drug delivery [22]. Among these compounds, tartronic acid is a high value-added chemical with high biological activity used in the treatment of metabolic disorders, liver diseases, and osteoporosis. It is also an anti-corrosive protective agent and a monomer of biopolymers [23–26].

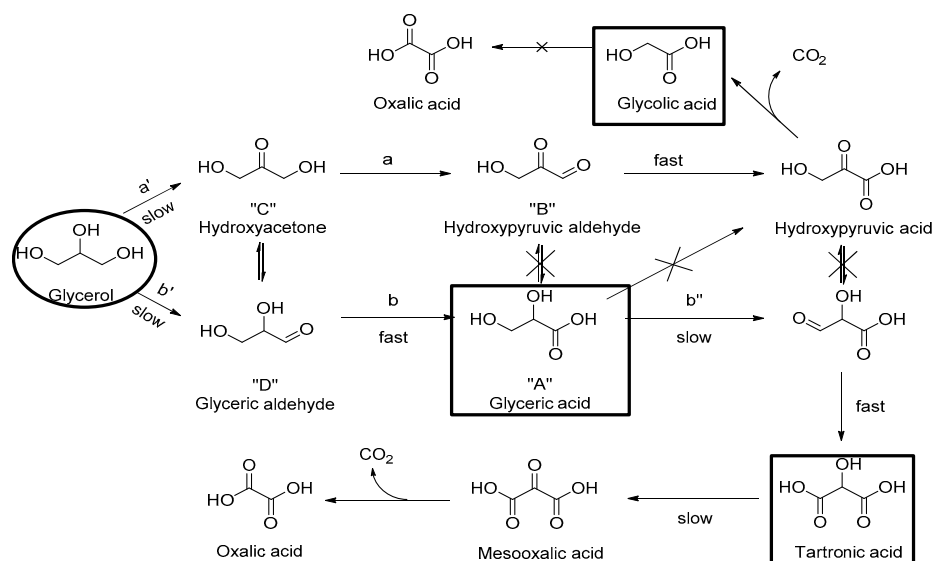
Table 1 briefly summarizes some of the catalytic results from research [27–35] on glycerol oxidation with molecular oxygen under pressure over gold supported catalysts in the presence of a base under different reaction conditions.

Carretin et al. [27] reported the selective oxidation of glycerol to glyceric acid (100% selectivity), probably via the initial formation of glyceraldehydes using gold supported on activated carbon or graphite under mild reaction conditions after 3 h. It was also noted that, with high concentrations of NaOH, exceptionally high selectivity to glyceric acid can be obtained. However, by decreasing the glycerol to gold ratio (R) from 540 to 214 and the oxygen concentration, an increase of glycerol conversion is obtained, with the formation of some tartronic acid via consecutive oxidation.

Table 1. Catalytic oxidation of glycerol on gold catalysts under basic conditions using O₂ as an oxidant and H₂O as a solvent.

Catalyst	<i>p</i> O ₂ , atm	<i>T</i> , °C	NaOH eqv.	Reaction Time, h	R ^a	Conversion, %	Selectivity, %			Ref.
							Glyceric Acid	Glycolic Acid	Tartronic Acid	
1% Au/Active carbon (AC)	3	50	1	3	538	56	100	0	0	[27]
1% Au/Graphite	3	60	2	3	538	54	100	0	0	[27]
1% Au/Graphite	3	60	1	3	540	43	80	0	20	[27]
1% Au/Graphite	6	60	2	3	214	91	92	0	6	[27]
1% Au/AC Cit-calc ^b	3	30	4	6	500	90	92	No info	No info	[28]
1% Au/AC Cit-calc	3	60	1	20	500	99	89	No info	No info	[28]
1% Au/AC PVA ^c	3	60	1	6	500	99	45	No info	No info	[28]
1.5% Au/AC	3	60	4	9	150	90	89	-	7	[29]
1.5% Au/CeO ₂	3	60	4	9	150	98	2	-	25	[29]
1.5% Au/NaY ^d	3	60	4	9	150	98	27	-	44	[29]
1.5% Au/REY ^d	3	60	4	9	150	99	5	-	70	[29]
1.5% Au/HY ^d	3	60	4	9	150	98	3	-	82	[29]
1% Au/TiO ₂	3	50	4	4	1000	68	81	3	5	[30]
1% Au/NiO	3	50	4	4	1000	99	55	11	9	[30]
1% Au/CNF-PS ^e	3	50	4	4	1000	64	55	22	-	[31]
1% Au/CNF-HT ^f	3	50	4	4	1000	70	22	35	-	[31]
1% Au-Nb ₂ O ₅	6	60	2	15	980	94	43	7	5	[32]
1% Au-Nb ₂ O ₅	6	60	2	5	980	67	47	5	5	[32]
2% Au-Nb ₂ O ₅	6	60	2	5	500	51	87	3	3	[33]
1% Au/CMK-3 ^g	7	60	4	5	500	82	71	15	8	[34]
1% Au/NCCR-56 ^g	7	60	4	5	500	84	70	17	7	[34]
1.6% Au/TiO ₂	11	60	2	3	8000	83	61	34	3	[35]
1.6% Au/TiO ₂	11	60	2	3	2000	91	63	14	13	[35]
1.6% Au/TiO ₂	11	60	2	3	350	100	50	7	25	[35]

^a R—Glycerol/Au ratio (mol/mol); ^b Citrate-protected gold sol preparation; ^c polyvinyl alcohol-protected gold sol preparation; ^d different type of Y zeolites; ^e Carbon nanofibers (CNF) produced by pyrolytic stripping (PS); ^f Carbon nanofibers (CNF) produced by heat-treating (HT); ^g Ordered mesoporous carbon types.



Scheme 1. Possible reaction pathways for the oxidation of glycerol under basic conditions. Reprinted from Ref. [28], Copyright (2004), with permission from Elsevier.

Porta and Prati [28] obtained a high selectivity towards glyceric acid (92%) with a 90% conversion of glycerol on a Au/C catalyst by optimizing the temperature and a NaOH/glycerol ratio. The higher the temperature, the higher the amount of tartronic acid formed (however, no data on selectivity values were provided). Also, larger gold particles (30 nm size) that were obtained with immobilization methods, maintained constant selectivity while particles with a smaller mean size (6 nm) obtained with incipient wetness or impregnation methods showed higher activity with a rapid change in selectivity. Besides that, the authors established the existence of two main pathways one leading to hydroxyacetone and glyceric aldehyde as the main oxidation products, and the other to glycolic and oxalic acids as the final compounds. In addition, the rapid oxidation of glyceraldehyde favors the formation of glyceric acid, rather than that of hydroxyacetone (Scheme 1).

Cai et al. [29] observed high catalytic performance (90–99% conversion after 9 h) in glycerol oxidation with different selectivity values on Au NPs deposited on various supports (CeO₂, activated carbon and different Y type zeolites). However, it should be noted that a low ratio of glycerol to Au (R = 150) was used in all cases. Preferential formation of tartronic acid (from 44 to 82%) was observed when Y type zeolite was used as the support, while the primary products on Au/CeO₂ and Au/C were oxalic acid (55%) and glyceric acid (89%), respectively. The authors proposed that the main reason for the formation of tartronic acid was the small size of the Au nanoclusters (1 nm) on the HY zeolite support.

Villa et al. [30] described high activity (full conversion) of PVA protected Au nanoparticles (NPs) supported on NiO for glycerol oxidation, but with lower selectivity (55%) to glycerate after 4 h of reaction. Under the same reaction conditions, Au/TiO₂ prepared the same way achieved 81% of glycerate selectivity but 64% for glycerol conversion. The improvement in activity by using NiO as the support was related to the stronger interaction between the support and the Au NPs. The XPS measurements revealed only Au⁰ species on both support (NiO and TiO₂) surfaces.

Wang et al. [31], investigated Au catalysts supported on nanofibers with different degrees of graphitization under the same reaction conditions used in [30]. They found a similar size of Au NPs (3.5–3.8 nm) with a similar level of activity in glycerol oxidation (64–70%), but with different product distributions. The authors attributed this to the different shape and configuration of the Au particles. On Au/CNF-PS, 55% of glyceric acid (C3 product) and 45% of formic and glycolic acid (C1 + C2 products) were obtained, while 22% of glyceric acid and 77% of formic and glycolic acid were observed using Au/CNF-HT. The high selectivity of the latter catalyst to C1 and C2 products, which derives from

the C-C bond cleavage, was supposedly associated with the exposure of low index Au planes surfaces caused by the direct contact between CNF-HT and the {111} surface of PVA Au NPs, while disordered carbon nanofiber surfaces (CNF-PS) led to random orientation of supported particles.

Sobczak et al. [28] obtained a Au/Nb₂O₅ catalyst with catalytic properties comparable to Au/C, prepared by the gold-sol method and crystalline niobia. After 5 h, glycerol conversion was 67% with glyceric acid as the main product. However, Au on carbon showed a different behavior. Thus, it was concluded that oxidation of glycerol is a complex process and many parameters influence the activity and selectivity of the catalysts used. Au/Nb₂O₅ was also tested in a second glycerol oxidation run by simple solvent decantation after the first run, without any drying and washing, and a small decrease in the activity (9%) with no change in selectivity was observed. Total selectivity (<100%) could not be reached for several reasons: polymerization of the reaction products, oxidation of the reaction products to CO₂ or adsorption of the products on the support surface. It was noted that glycolic acid formation proceeds via cracking of the C-C bond by the acidic centers on the catalyst surface. The authors suggested that the higher yield of tartronic acid was caused by the slow desorption of glyceric acid. The Au-Nb₂O₅ catalyst was also investigated by Wolski [33], who found that with Au NPs smaller than 3 nm, the catalyst ability of C-C bond cleavage was enhanced and promoted formation of C2 and C1 products.

Murthy and Selvam [34] reported 82–84% glycerol conversion after 5 h on mesoporous carbon supported nano-gold catalysts synthesized by the sol-immobilization method, with 70% selectivity to glyceric acid. The remarkable performance of both fresh and regenerated catalysts (second cycle), was attributed to the presence of pore channels in mesoporous carbons, which act as nanoreactors preventing the agglomeration of nanoparticles.

Zope et al. [35] studied the factors that influence the formation of diacids (tartronic and oxalic acids) in glycerol oxidation and of furandicarboxylic acid in 5-hydroxymethylfurfural (HMF) oxidation over gold supported catalysts (Au/TiO₂ and Au/C). Interestingly, hydrotalcite was used as an alternative to liquid bases for HMF reaction, which requires further neutralization. To effectively produce diacids, the use of a continuous reactor or high Au catalyst loadings in a semi-bath reactor was needed. Such conditions are necessary to prevent the formation of trace byproduct species from monoacid, since such species inhibit the rate of both glycerol oxidation and monoacid oxidation to diacid. Thus, the best results were obtained in the semi-bath reactor with R = 350: full conversion and 30% of diacid (25% of tartronic acid and 5% of oxalic acid) over Au/TiO₂ catalyst after 3 h at 60 °C under 11 bar of O₂.

After analyzing these works, it can be concluded that it is essential to control the activity and selectivity in the process of liquid-phase oxidation of glycerol, and a comprehensive approach is necessary. This includes taking into account the particle size and shape of gold, the choice of the support and reaction conditions, that is, the amount of base and gold added relative to alcohol, and reaction temperature.

The aim of this work was to study the influence of the nature of the support and the base additives on the catalytic performance of gold catalysts in the liquid phase oxidation of glycerol by molecular oxygen.

2. Materials and Methods

Gold catalysts with a nominal load of 4% were prepared, using HAuCl₄·4H₂O (Merck, Darmstadt, Germany) as a precursor, using the deposition-precipitation with urea (Merck, Darmstadt, Germany) method. Commercial oxides TiO₂, CeO₂, La₂O₃ and MgO (Aldrich), and titanium oxide modified by impregnation with aqueous solutions of La(NO₃)₃·6H₂O, Ce(NO₃)₃·6H₂O or Mg(NO₃)₂·6H₂O (Merck, Darmstadt, Germany) in a molar ratio Ti/M (La, Ce, Mg) = 40, according to the procedure described in previous works [36–38], were used as supports.

Pretreatment in a hydrogen atmosphere for 1 h at a temperature of 300 °C was used for the decomposition of the products of the hydrolysis of the complex of gold (III) with urea on the support surface [39].

The catalysts were characterized by adsorption-desorption of N₂ at −196 °C on a Micromeritics 23x-Tristar 3000 Apparatus, Micromeritics Instrument Corporation (Norcross, GA, USA), X-ray diffraction (XRD) on a Philips XPert PRO diffractometer (Amsterdam, Netherlands), X-ray photoelectron spectroscopy (XPS), on a ESCALAB 200A, VG Scientific (Waltham, MA, USA), energy-dispersive X-ray spectroscopy (EDX), transmission electron microscopy (TEM), as well as scanning transmission electron microscopy-high angle annular dark field (STEM-HAADF) using one single microscope (JEOL JEM-2100F, JEOL Ltd., Tokyo, Japan) and the temperature-programmed carbon dioxide (CO₂-TPD) method on a “Chemosorb” chemisorption analyzer (Neosib, Novosibirsk, Russia) as previously reported in [36–38,40–42], where the detailed description of the applied procedures can be found.

The size of the gold NPs used in the (i.e., after the reaction test) catalysts was investigated by high resolution transmission electron microscopy (HRTEM) using a JEM-2100F instrument. The samples were ground to a fine powder and sonicated in hexane at room temperature. Then, a part of the suspension was placed on a lacey carbon-coated Cu grid. For each sample, at least 300 particles were counted.

The determination of the basic sites is described in detail in previous papers by our group [37,38]. Briefly, the CO₂-temperature-programmable desorption (TPD) method was applied using a “Chemosorb” chemisorption analyzer (Neosib, Novosibirsk, Russia), equipped with a thermal conductivity detector (TCD). After treatment in an inert atmosphere, samples were saturated with CO₂ for 1 h at 25 °C and the temperature was increased to 600 °C at a rate of 10 °C min^{−1} under an inert atmosphere. Total basicity was calculated from the area of the desorption peaks.

The catalytic tests were carried out in a semi-batch reactor operated under 3 atm of oxygen at 50 °C under stirring at 1100 rpm. Typically, the catalyst sample was added in a glycerol/gold ratio R = 1000 mol/mol to 10 mL of 0.3 M glycerol (87 wt.% solution, Fluka, Maurice, NJ, USA) and 1.2 M NaOH aqueous solution (distilled water) in a glass reactor equipped with heater, mechanical stirrer, gas supply system and thermometer. Small aliquots of the reacting mixture were taken after 15, 30, 60, 120 and 180 min to monitor the reaction progress. Catalytic experiments with alkaline earth bases (MgO, SrO, CaO) were performed with Au/La₂O₃/TiO₂ catalyst under the conditions described above (R = 1000, pO₂ = 3 atm) with different glycerol/base molar ratios (4 or 12) and reaction temperatures (50, 80 or 95 °C), over a 6 h period.

The reactants and products were analyzed and quantified by high-performance liquid chromatography (HPLC, Agilent Technologies, 1220 Infinity, Santa Clara, CA, USA) using a column Alltech OA-10308 (L × i.d.: 300 mm × 7.8 mm, Fisher Scientific, Hampton, NH, USA) with ultraviolet (Varian 9050 UV, 210 nm) and refractive index (Waters RI) detectors, using 0.4 mL/min of 0.1% aqueous solution of H₃PO₄ as the eluent. Attribution of peaks was made by comparison with chromatograms of standard samples. No activity of oxidation of glycerol was observed in the absence of support/catalyst.

The conversion of glycerol and selectivity to products were calculated in terms of moles of C atoms, according to Equations (1) and (2), respectively:

$$\text{Conversion (\% mol)} = \frac{\text{C moles of all products}}{\text{C moles of glycerol}} \times 100 \quad (1)$$

$$\text{Selectivity (\% mol)} = \frac{\text{C moles of product formed}}{\text{C moles of all products}} \times 100 \quad (2)$$

Turnover frequency (TOF) was calculated with regard to the number of moles of gold during the first 15 min as follows:

$$\text{TOF (h}^{-1}\text{)} = \frac{\text{Conversion after 15 min} \times \text{initial moles of glycerol}}{\text{moles of Au} \times 100 \times 0.25 \text{ h}} \quad (3)$$

The carbon balance in all the reported test data was within 100 ± 5%.

3. Results and Discussion

3.1. Catalytic Results

In our previous work [36,37,40], we found that for alcohol oxidation on gold supported catalysts, the optimal gold content was 4 wt.% and the optimal pretreatment was a reducing atmosphere. For this reason, glycerol oxidation was investigated on samples with 4 wt.% Au after pretreatment in H₂ (Figure 1).

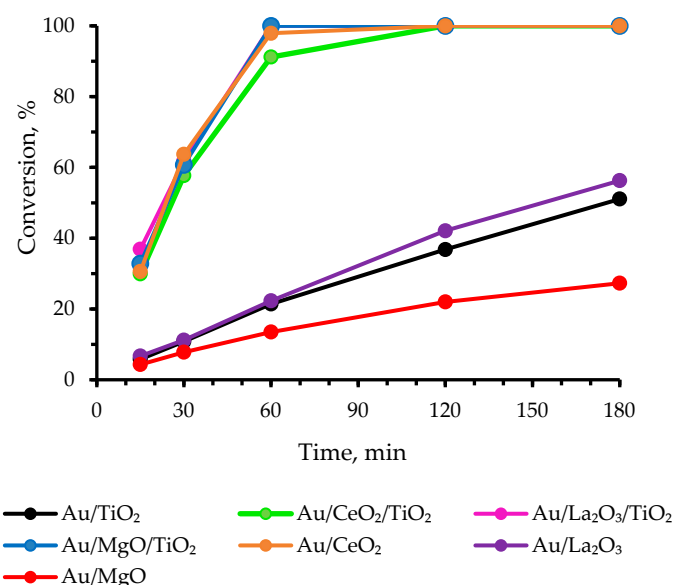


Figure 1. Effect of the nature of the support on the oxidation of glycerol on Au/MxO_y catalysts: evolution of conversion with run time. Reaction conditions: T = 50 °C, 0.3 M Glycerol (H₂O), NaOH/glycerol = 4 eqv., R = 1000, stirring rate = 1100 rpm.

It can be seen that samples of Au on modified titanium oxides and pure cerium oxide were extremely active. The full conversion of glycerol was observed after only 1 h on Au/MgO/TiO₂ and Au/La₂O₃/TiO₂ catalysts, and after 2 h on Au/CeO₂/TiO₂ and Au/CeO₂ samples. Au/La₂O₃ and Au/TiO₂ showed almost the same behavior with regard to the progress of the conversion with run time, and obtained a 51–56% conversion rate after 3 h. The least active sample was Au/MgO with a 27% conversion after 3 h.

In terms of TOF, after 15 min (Table 2) the order of the catalyst's initial activity in glycerol oxidation was: Au/MgO/TiO₂ ≥ Au/La₂O₃/TiO₂ > Au/CeO₂ > Au/CeO₂/TiO₂ > Au/La₂O₃ > Au/TiO₂ > Au/MgO.

Table 2. Catalytic performance of gold-supported catalysts ^a.

Entry	Catalyst	TOF ^b	Conv. %	Selectivity at the Highest Conversion, %					
				Glyceric Acid	Glycolic Acid	Tartronic Acid	Formic Acid	Lactic Acid	Oxalic Acid
1	Au/TiO ₂	223	51	66	14	4	9	5	2
2	Au/CeO ₂ /TiO ₂ ^c	1186	100	44	14	24	8	6	4
3	Au/CeO ₂ /TiO ₂ ^d	1186	100	38	13	32	7	5	4
4	Au/CeO ₂	1225	100	67	9	12	5	6	1
5	Au/La ₂ O ₃ /TiO ₂	1277	100	68	11	8	4	8	1
6	Au/La ₂ O ₃	264	56	71	11	3	8	6	1
7	Au/MgO/TiO ₂	1295	100	56	12	15	7	8	2
8	Au/MgO	176	27	60	17	3	12	7	1

^a Reaction conditions: T = 50 °C, 0.3 M Glycerol (H₂O), NaOH/glycerol = 4 eqv., R = 1000, 1100 rpm stirring rate;

^b TOF calculated after 15 min; ^c Selectivity after 2 h; ^d Selectivity after 3 h. Conv. – conversion.

In all cases, the main product was glyceric acid (38–77% selectivity) with some formation of glycolic, tartronic, formic, lactic and oxalic acids, after 3 h of the reaction (Figure 2). The exception in the selectivity trends was the Au/CeO₂/TiO₂ sample, where a higher amount of tartronic acid (up to

32%) was formed (Table 2, entry 7). It is also worth noting that with increasing time, for all of the active samples the selectivity changes towards the formation of tartronic acid as a product of the oxidation of glyceric acid (Figure 2b–d,f).

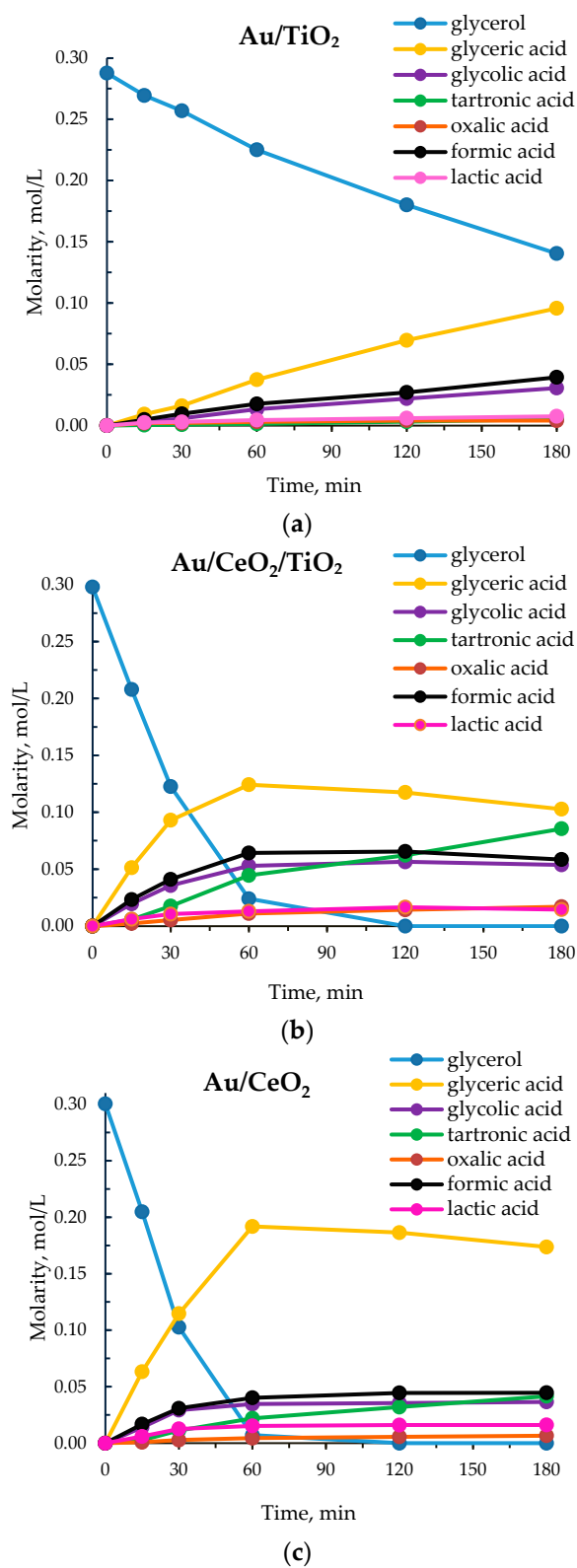
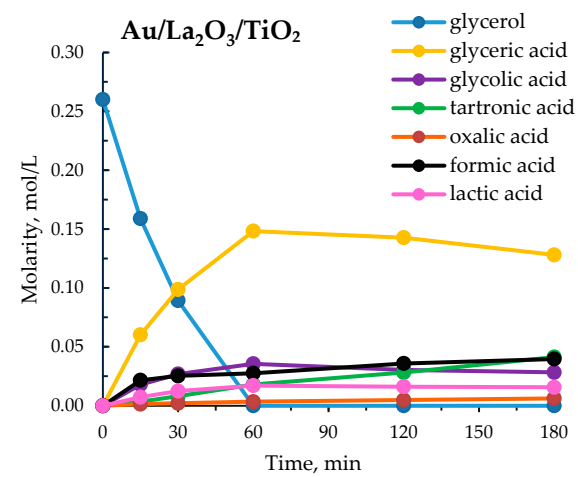
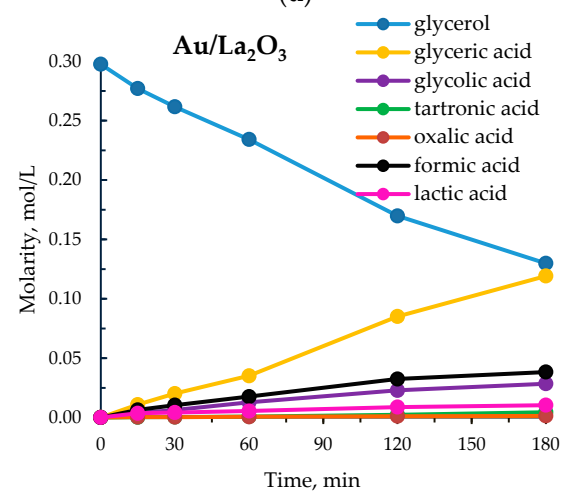


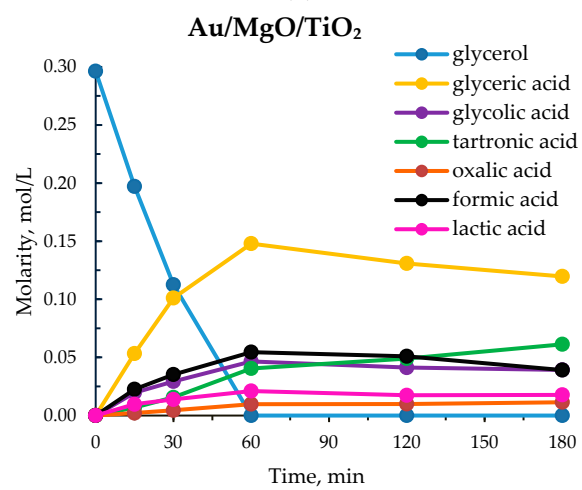
Figure 2. Cont.



(d)



(e)



(f)

Figure 2. Cont.

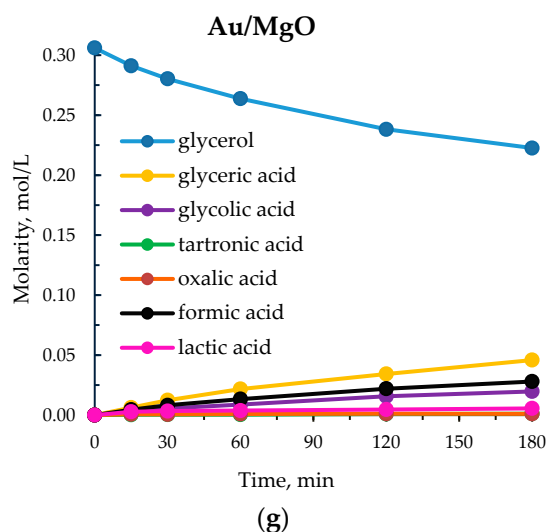


Figure 2. Product distribution in glycerol oxidation on gold supported catalysts (a–g). Reaction conditions: T = 50 °C, NaOH/glycerol = 4 eqv., R = 1000, 1100 rpm of stirring rate.

It should be mentioned that for all catalysts, only 2–5% of glycerol conversion was observed in the absence of bases (R = 500, T = 80 °C, 6 h).

3.2. Study of the Influence of Alkaline Earth Base Additives

The above results show the efficiency of our catalysts in the presence of alkali in comparison with the other gold supported materials presented in Table 1. However, from an industrial point of view, there is a major technical advantage when base-free conditions are used, that is, the formation of free carboxylic acid instead of the corresponding salts, particularly when sodium hydroxide is applied. Since we observed that our catalysts had very low activity in the absence of NaOH, we replaced it with alkaline earth bases such as MgO, CaO and SrO in order to obtain free carboxylic acids (Table 3). Au/La₂O₃/TiO₂ (one of the most active catalysts in this study) was used for these experiments.

Table 3. Effect of an alkaline earth base and reaction temperature on glycerol oxidation on Au/La₂O₃/TiO₂^a.

Entry	Alkaline Earth Base	T, °C	Gly/Base	Conv. %	Selectivity, %				
					Glyceric Acid	Glycolic Acid	Tartronic Acid	Formic Acid	Oxalic Acid
1	SrO	50	12	7	48	22	4	26	0
2	MgO	50	12	10	48	27	8	11	6
3	CaO	50	12	8	48	23	4	25	0
4	SrO	80	12	9	53	23	4	20	1
5	MgO	80	12	14	53	27	5	9	6
6	CaO	80	12	13	40	29	3	28	0
7	MgO	80	4	16	56	27	10	0	7
8	MgO	95	4	20	52	29	12	0	7
9	MgO ^b	95	4	0.4	100	0	0	0	0
10	No base	95	0	2	54	0	0	46	0

^a Reaction conditions: 0.3 M Glycerol (H₂O), 3 atm of O₂, R = 1000, 1100 rpm stirring rate; 6 h. ^b In the absence of catalyst. Gly.—glycerol, Conv.—conversion.

As can be seen in Table 3, the order of activity, in terms of conversion, was MgO > CaO > SrO. In particular, the addition of alkaline earth bases had a positive effect on the activity, especially when MgO was used. In all cases, higher temperatures led to an increase in the conversion of glycerol (Table 3, 3rd column).

The product distribution showed that a larger quantity of glyceric acid was formed when glycolic acid was the second product. Moreover, on SrO and CaO, formic acid formed in approximately equal amounts as the glycolic acid (20–28%). Small quantities of tartronic and oxalic acid were determined

as well. When MgO was added, the formic acid disappeared, resulting in higher conversion values (Table 3, entries 7 and 8).

Although full conversion of glycerol was not achieved, the use of alkaline earth bases is definitely advantageous compared to that of NaOH, since it promotes free carboxylic acids formation instead of corresponding salts. Also, we can assume that a higher performance could be obtained with proper development of the catalyst composition and reaction conditions.

3.3. Catalyst Characterization

The characterization of the samples used in this work is reported in our previous papers [36–38,40–42] and this is summarized in Table 4.

Table 4. Physicochemical characterization data for supports and the corresponding gold catalysts. Adapted from [36–38,40–42].

Entry	Sample	S_{BET} , m ² /g		EDX Au Content, wt. %	Au average Particle Size, nm	Au Relative Content, %			
		Catalyst	Support			Au ⁰	Au ¹⁺	Au ³⁺	Au _n ^{δ-}
1	Au/TiO ₂	50	55	4.0	3.0	75	14	11	0
2	Au/CeO ₂ /TiO ₂	46	48	4.1	2.8	68	20	12	0
3	Au/CeO ₂	38	37	4.3	2.6	57	21	0	22
4	Au/La ₂ O ₃ /TiO ₂	43	48	3.3	2.6	83	17	0	0
5	Au/La ₂ O ₃	10	9	4.5	3.6	50	12	0	38
6	Au/MgO/TiO ₂	43	48	4.0	5.1	51	29	20	0
7	Au/MgO	312	141	3.9	6.1	100	0	0	0

XRD analysis of Au catalysts and the corresponding supports [37,38,42] (Figure S1) showed no alteration in the phase composition or the support structure after gold loading, except: (1) Au/La₂O₃ (Figure S1e), which showed peaks related to La(OH)₃ (hexagonal) and La₂(CO₃)₂(OH)₂ (orthorhombic) [38]; and (2) Au/MgO (Figure S1g), where transformation of the oxide to hydroxide Mg(OH)₂ occurred [42]. Additionally, no peaks related to Au were found, indicating either the small size of the Au particles and metal oxides or their amorphous structure. The metallic gold phase was found only in the case of the Au/MgO sample, with an average crystal size of 3.1 nm [42].

In all cases, the Au content detected by EDX analysis was close to the nominal one (Table 4). N₂ adsorption-desorption revealed no significant changes in the specific surface area after gold deposition on each support, except Au/MgO, where a 2.2-fold increase in S_{BET} was found for MgO after gold addition, which is consistent with the changes in the support structure and composition revealed by XRD (Figure S1g).

The mean particle size of gold as determined by HRTEM varied from 2.4 to 5.1 nm for modified titania samples, while gold on pure oxides was in the range of 2.6–6.1 nm (Figure S2). In contrast to numerous studies on the oxidation of glycerol that show the direct dependence of the catalytic activity on the average size of the Au NPs (the smaller the NPs size, the higher the activity) [28,31,33,34], this trend was not observed in the present work (Figure 3).

For example, the two most active catalysts, Au/MgO/TiO₂ and Au/La₂O₃/TiO₂ have similar TOF values (Table 2), but they have different average particle size of 5.1 and 2.6 nm, respectively. Another example is the comparison of Au/TiO₂ and Au/MgO/TiO₂ (Figure 3). Thus, it can be assumed that the average size of the Au NPs is not the only determining factor.

The XPS results showed the presence of gold in four different electronic states: metallic (Au⁰), monovalent (Au⁺), trivalent (Au³⁺) and electronegative (Au_n^{δ-}) (Table 4, Figure S3). No correlation was found between the surface concentration of the gold states and the catalytic data.

It is known that the basic properties of catalysts play an important role in the oxidation of alcohols. To assess their impact, CO₂ temperature-programmed desorption experiments were carried out for both the catalysts and supports (Table 5) [37,38].

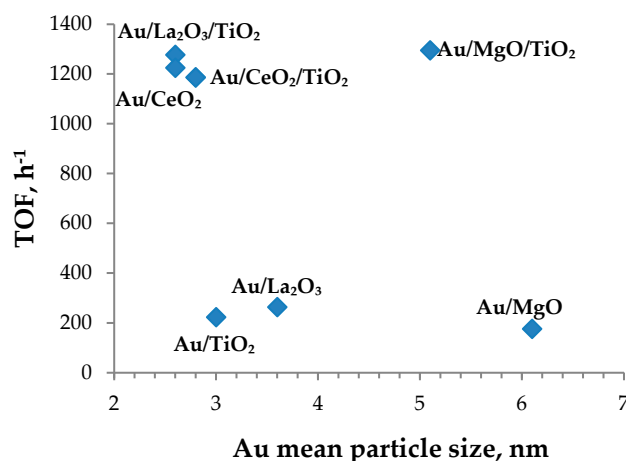


Figure 3. Turnover frequency (TOF) in glycerol oxidation for gold supported catalysts as a function of gold mean particle size.

Table 5. Basic properties of the catalysts and corresponding supports, TOF values and mean particle size (D_{mean}) of the catalysts. Adapted from [37,38], except the data for MgO-based catalysts (entries 6 and 7), which is presented for the first time in this paper.

Entry	Sample	Concentration of Base Sites, $\mu\text{mol/g}$, %		TOF, h^{-1}	D_{mean} , nm
		Support	Catalyst		
1	Au/TiO ₂	88	73	223	3.0
2	Au/CeO ₂ /TiO ₂	70	153	1186	2.8
3	Au/CeO ₂	122	230	1225	2.6
4	Au/La ₂ O ₃ /TiO ₂	119	161	1277	2.6
5	Au/La ₂ O ₃	84	1523	264	3.6
6	Au/MgO/TiO ₂	191	236	1295	5.1
7	Au/MgO	409	665	176	6.1

TiO₂, CeO₂/TiO₂, and La₂O₃ supports possess weak basic properties, CeO₂ and La₂O₃/TiO₂ supports have an average number of basic centers, and supports with magnesium, MgO/TiO₂ and especially MgO, have a strong basicity, as expected (Table 5, 3rd column).

After the deposition of gold, an increase in the general basicity was observed for all samples (Table 5, 4th column), except Au/TiO₂. This means that a redistribution of the base centers occurred due to the interaction of the gold precursor, urea and/or water with the support during the preparation of the catalyst [38,41]. For Au/MgO, and especially Au/La₂O₃, the increased basicity was associated with a complete change in the phase composition, which can be explained by the chemical properties of these supports, and exhibited in the interaction with water and urea hydrolysis products, during the preparation of the catalyst. Namely, for Au/MgO, the transition of the oxide to the hydroxide led to an increase of the Brønsted base centers (OH groups). For Au/La₂O₃, the presence of lanthanum hydroxycarbonate along with lanthanum hydroxide complicated an evaluation of the base sites for this sample due to the contribution of residual carbonates to the total release of CO₂ in addition to CO₂ desorbed from the base sites [38]. The highest basicity values (230–236 $\mu\text{mol/g}$) were observed for Au/CeO₂ and Au/MgO/TiO₂, which showed an increase in the total basicity of 1.9 and 1.2 times, respectively, compared to the concentration of base sites for CeO₂ and MgO/TiO₂. After the deposition of gold on CeO₂/TiO₂ and La₂O₃/TiO₂, the number of base centers increased 2.2 and 1.5 times, respectively, and the corresponding catalysts had approximately the same basicity level (153–161 $\mu\text{mol/g}$). A comparison of the obtained basicity results with TOF (Tables 2 and 4) did not reveal a direct correlation between the concentration of basic centers and the activity of the studied catalysts in glycerol oxidation (Figure 4).

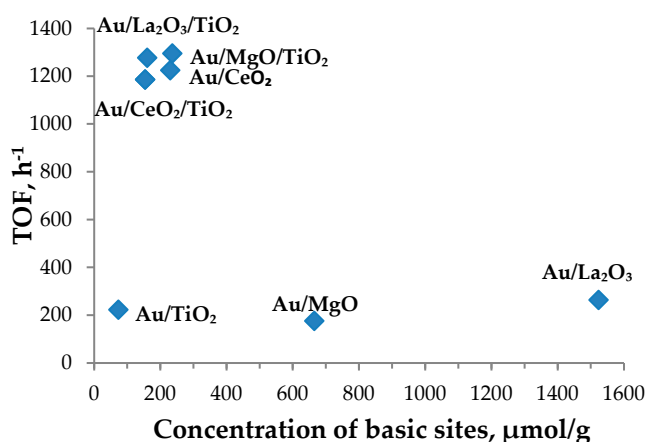


Figure 4. Concentration of basic sites and TOF in glycerol oxidation for gold supported catalysts.

However, if the TOF results are compared with the average particle size and total basicity, it is clear that samples with Au nanoparticles smaller than 2 nm and a high amount of base sites have the highest TOF values. Although Au/MgO/TiO₂ is characterized by a small number of small particles and has one of the highest average sizes (5.1 nm), it had the largest TOF among all catalysts after 15 min of the reaction due to its high basicity (236 $\mu\text{mol/g}$). It is likely that the role of the basic groups of the support, as in the case of added NaOH, is to enable faster deprotonation of glycerol, thereby facilitating the primary oxidation step. Prior to the deprotonation, adsorption of glycerol and oxygen and the further oxidation of the alcohol after activation of the hydroxyl group by the base occur on gold [43,44], depending on its distribution and size on the surface of the support. So, although Au/CeO₂ has half the average gold size of Au/MgO/TiO₂, it showed an initial TOF value smaller than that of Au/MgO/TiO₂ because Au/CeO₂ has fewer basic centers compared to Au/MgO/TiO₂. This also explains why Au/TiO₂, with a size of 3 nm showed medium activity, as this catalyst has the lowest basicity. Unfortunately, it was not possible to directly assess the basicity of Au/La₂O₃ because of the presence of carbonates and higher average particle size (3.6 nm); therefore, we cannot draw definite conclusions for this sample. It should also be taken into account that the specific surface of this sample was the smallest (Table 4), which can also affect its catalytic performance. Finally, Au/MgO has the lowest TOF value, which can be explained by the fact that it has the largest Au NPs size.

Thus, we can conclude that a combination of small particle size and high concentration of basic groups is necessary for the effective oxidation of glycerol over gold supported catalysts.

However, there still remains an unanswered question as to why Au/CeO₂/TiO₂, which has the lowest TOF among the active catalysts, shows the highest yield of tartronic acid, a product of the oxidation of glyceric acid, as observed in the reaction products.

Perhaps, as many authors have noted [29,45–47], deeper oxidation of glycerol occurs with the formation of tartronic acid, and products associated with the cleavage of the C-C bond of glycerol are formed (formic, glycolic and oxalic acids) when small particles of gold (smaller than 2 nm) are present. In order to better study the effect of the Au NPs size and assess whether the gold distribution changed after the reaction, we performed HRTEM of the samples in which high TOF values were achieved (Au/CeO₂/TiO₂, Au/CeO₂, Au/La₂O₃/TiO₂ and Au/MgO/TiO₂) (Figure 5). An EDX analysis was also performed in parallel, and no leaching of gold was detected after the reaction. However, for all catalysts, except Au/CeO₂/TiO₂, there was a noticeable increase in the average particle size after the reaction, as compared with the corresponding values before the reaction (Table 6). Such particle growth may indicate some deactivation of the catalysts, which prevents the further oxidation of glyceric acid to tartronic acid. Indeed, some tendencies were observed including the smaller the particle growth observed, the higher the amount of tartronic acid formed.

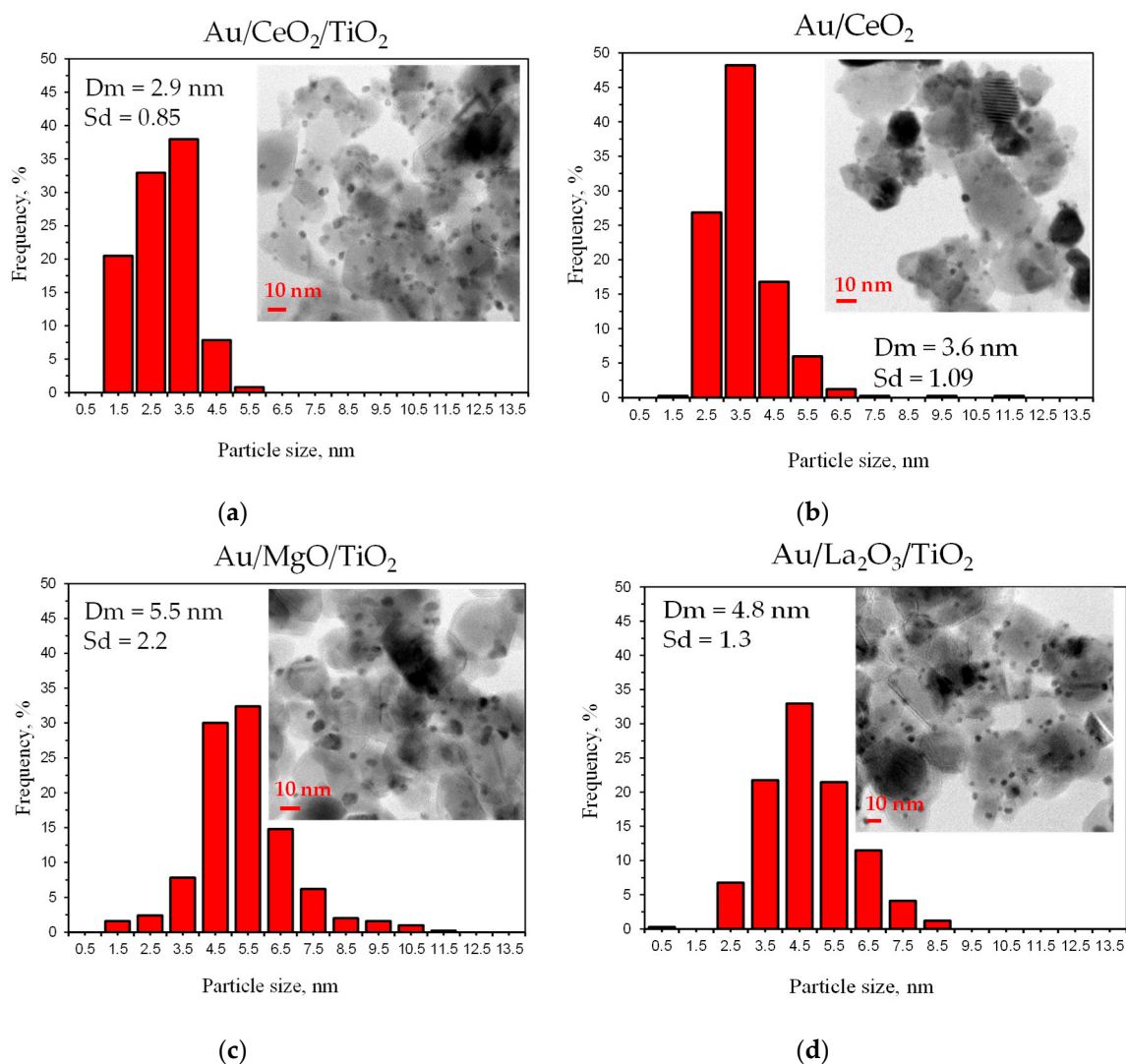


Figure 5. HRTEM images and the particle size distribution of the used gold catalysts after glycerol oxidation reaction ($T = 50\text{ }^{\circ}\text{C}$, 0.3 M Glycerol (H_2O), $\text{NaOH/glycerol} = 4\text{ eqv.}$, $R = 1000, 1100\text{ rpm}$ stirring rate, 3 h).

Table 6. Comparison of mean diameter of gold catalysts before and after glycerol oxidation reaction.

Entry	Sample	Average Particle Size		Selectivity (%) towards Tartronic Acid after 3 h
		Before a Reaction	After Glycerol Oxidation	
1	Au/CeO ₂ /TiO ₂	2.8	2.9	32
2	Au/MgO/TiO ₂	5.1	5.5	25
3	Au/CeO ₂	2.6	3.6	19
4	Au/La ₂ O ₃ /TiO ₂	2.6	4.8	15

4. Conclusions

The efficiency of gold catalysts supported on pure oxides (TiO_2 , CeO_2 , La_2O_3 and MgO) or modified titania ($\text{CeO}_2/\text{TiO}_2$, $\text{La}_2\text{O}_3/\text{TiO}_2$ and MgO/TiO_2) was investigated in the aerobic oxidation of glycerol under mild ($T = 50\text{ }^{\circ}\text{C}$, 3 atm of O_2 and added base) conditions.

Gold catalysts were highly effective in the oxidation of glycerol in the presence of an alkaline base (NaOH). The order of the catalyst's initial activity (TOF in 15 min) was found to be as follows: $\text{Au/MgO}/\text{TiO}_2 \geq \text{Au/La}_2\text{O}_3/\text{TiO}_2 > \text{Au/CeO}_2 > \text{Au/CeO}_2/\text{TiO}_2 > \text{Au/La}_2\text{O}_3 > \text{Au}/\text{TiO}_2 > \text{Au/MgO}$.

A combination of small particle size and high concentration of basic groups was proposed as requisite for the effective oxidation of glycerol.

The main product was sodium glycerate (38–72%). However, on the most active catalysts (Au/La₂O₃/TiO₂, Au/CeO₂, Au/MgO/TiO₂ and Au/CeO₂/TiO₂) that exhibited full conversion, an increase in the formation sodium tartronate was observed with run time, and the selectivity to tartronate on these materials after 3 h (glycerol/Au = 1000) was as follows: 15, 19, 25 and 32% respectively. The tendency of these catalysts is as follows: the higher the growth of Au NPs after the reaction, the less formation of tartronate, which may indicate some deactivation of the catalysts, which prevents the further oxidation of glyceric acid to tartronic acid.

Although replacing traditional alkaline base (NaOH) with alkaline earth bases (CaO, SrO and MgO) did not provide higher activity, it led to the formation of free carboxylic acids in contrast to the salts formed in the case of NaOH. The highest conversion of 20% was achieved when MgO and Au/La₂O₃/TiO₂ catalyst were used, giving a 52% selectivity to glyceric acid in 6 h at T = 95 °C, glycerol/MgO = 4 and glycerol/Au = 1000.

Supplementary Materials: The following are available online at <http://www.mdpi.com/2227-9717/8/9/1016/s1>, Figure S1: XRD patterns for different catalysts and their corresponding supports: (a–e) from [38], (f) from [37], g from [42]; Figure S2: TEM images and particle size distributions of gold supported catalysts: (a–e) from [38], (f) from [37], g from [42]; XPS results from different catalysts: (a–e) from [40], (f) from [37], g from [42].

Author Contributions: E.P. carried out the preparation and pretreatment of the catalysts, performed the catalytic tests with NaOH, and wrote the first draft of the paper; E.K. was responsible for the methodology of the catalytic tests with alkaline earth base additives, supervised those experiments and participated in the writing; M.S., A.V. and L.P. dealt with the methodology of catalytic tests with NaOH; D.G. was responsible for the catalytic results with alkaline earth base additives; M.S., A.V., L.P., S.A.C.C., N.B., V.C.C. and A.P. provided the means for the realization of this work and contributed to the supervision and paper revision. All authors read and approved the final manuscript.

Funding: This work was partially supported by the Associate Laboratory for Green Chemistry (LAQV), financed by national funds from FCT/MCTES (UIDB/50006/2020) (Portugal), the Tomsk Polytechnic University Competitiveness Enhancement Program project VIU-RSCBMT-197/2020, and the Russian Foundation of Basic Research, project 18-29-24037.

Acknowledgments: TEM analysis was carried out at the Innovation Centre for Nanomaterials and Nanotechnologies of Tomsk Polytechnic University.

Conflicts of Interest: The authors declare no conflict of interest.

References

1. Werpy, T.; Petersen, G. Top Value Added Chemicals from Biomass: Volume I—Results of Screening for Potential Candidates from Sugars and Synthesis Gas. Available online: <https://www.osti.gov/biblio/15008859-top-value-added-chemicals-from-biomass-volume-results-screening-potpotent-candidates-from-sugars-synthesis-gas> (accessed on 16 June 2020).
2. Chheda, J.N.; Huber, G.W.; Dumesic, J.A. Liquid-phase catalytic processing of biomass-derived oxygenated hydrocarbons to fuels and chemicals. *Angew. Chem. Int. Ed.* **2007**, *46*, 7164–7183. [[CrossRef](#)] [[PubMed](#)]
3. Christoph, R.; Schmidt, B.; Steinberner, U.; Dilla, W.; Karinen, R. Glycerol, Ullmann's Encyclopedia of Industrial Chemistry. Available online: https://onlinelibrary.wiley.com/doi/full/10.1002/14356007.a12_477.pub2 (accessed on 16 June 2020).
4. Glycerine: An Overview. Available online: https://www.aciscience.org/docs/Glycerine_-_an_overview.pdf (accessed on 16 June 2020).
5. Esposito, R.; Raucci, U.; Cucciolo, M.E.; Di Guida, R.; Scamardella, C.; Rega, N.; Ruffo, F. Iron(III) complexes for highly efficient and sustainable ketalization of glycerol: A combined experimental and theoretical study. *ACS Omega* **2019**, *4*, 688–698. [[CrossRef](#)] [[PubMed](#)]
6. Quispe, C.A.G.; Coronado, C.J.R.; Carvalho, J.A. Glycerol: Production, consumption, prices, characterization and new trends in combustion. *Renew. Sustain. Energy Rev.* **2013**, *27*, 475–493. [[CrossRef](#)]
7. Villa, A.; Dimitratos, N.; Chan-Thaw, C.E.; Hammond, C.; Prati, L.; Hutchings, G.J. Glycerol oxidation using gold-containing catalysts. *Acc. Chem. Res.* **2015**, *48*, 1403–1412. [[CrossRef](#)] [[PubMed](#)]

8. Dodekatos, G.; Schünemann, S.; Tüysüz, H. Recent advances in thermo-, photo-, and electrocatalytic glycerol oxidation. *ACS Catal.* **2018**, *8*, 6301–6333. [CrossRef]
9. The EU Biodiesel Industry. Available online: <https://www.ebb-eu.org/stats.php> (accessed on 16 June 2020).
10. Mallat, T.; Baiker, A. Oxidation of alcohols with molecular oxygen on platinum metal catalysts in aqueous solutions. *Catal. Today* **1994**, *19*, 247–283. [CrossRef]
11. Garcia, R.; Besson, M.; Gallezot, P. Chemoselective catalytic oxidation of glycerol with air on platinum metals. *Appl. Catal. A Gen.* **1995**, *127*, 165–176. [CrossRef]
12. Kimura, H.; Tsuto, K.; Wakisaka, T.; Kazumi, Y.; Inaya, Y. Selective oxidation of glycerol on a platinum-bismuth catalyst. *Appl. Catal. A Gen.* **1993**, *96*, 217–228. [CrossRef]
13. Mallat, T.; Baiker, A. Oxidation of alcohols with molecular oxygen on solid catalysts. *Chem. Rev.* **2004**, *104*, 3037–3058. [CrossRef]
14. Abad, A.; Almela, C.; Corma, A.; Garcia, H. Unique gold chemoselectivity for the aerobic oxidation of allylic alcohols. *Chem. Commun.* **2006**, 3178–3180. [CrossRef]
15. Villa, A.; Veith, G.M.; Prati, L. Selective oxidation of glycerol under acidic conditions using gold catalysts. *Angew. Chem. Int. Ed.* **2010**, *49*, 4499–4502. [CrossRef] [PubMed]
16. Carrettin, S.; McMorn, P.; Johnston, P.; Griffin, K.; Kiely, C.J.; Hutchings, G.J. Oxidation of glycerol using supported Pt, Pd and Au catalysts. *Phys. Chem. Chem. Phys.* **2003**, *5*, 1329–1336. [CrossRef]
17. Dimitratos, N.; Villa, A.; Bianchi, C.L.; Prati, L.; Makkee, M. Gold on titania: Effect of preparation method in the liquid phase oxidation. *Appl. Catal. A Gen.* **2006**, *311*, 185–192. [CrossRef]
18. Habe, H.; Fukuoka, T.; Kitamoto, D.; Sakaki, K. Biotechnological production of d-glyceric acid and its application. *Appl. Microbiol. Biotechnol.* **2009**, *84*, 445–452. [CrossRef] [PubMed]
19. Habe, H.; Fukuoka, T.; Kitamoto, D.; Sakaki, K. Application of electro dialysis to glycerate recovery from a glycerol containing model solution and culture broth. *J. Biosci. Bioeng.* **2009**, *107*, 425–428. [CrossRef]
20. Habe, H.; Fukuoka, T.; Kitamoto, D.; Sakaki, K. Biotransformation of glycerol to d-glyceric acid by *Acetobacter tropicalis*. *Appl. Microbiol. Biotechnol.* **2009**, *81*, 1033–1039. [CrossRef]
21. Yunhai, S.; Houyong, S.; Deming, L.; Qinghua, L.; Dexing, C.; Yongchuan, Z. Separation of glycolic acid from glycolonitrile hydrolysate by reactive extraction with tri-n-octylamine. *Sep. Purif. Technol.* **2006**, *49*, 20–26. [CrossRef]
22. Santiago, L.G.; Soccol, C.R.; Castro, G.R. Emerging technologies for bioactive applications in foods. In *Food Bioactives: Extraction and Biotechnology Applications*; Puri, M., Ed.; Springer International Publishing AG: Cham, Switzerland, 2017; pp. 205–226. ISBN 978-3-319-51637-0.
23. Katryniok, B.; Kimura, H.; Skrzyńska, E.; Girardon, J.-S.; Fongarland, P.; Capron, M.; Ducoulombier, R.; Mimura, N.; Paul, S.; Dumeignil, F. Selective catalytic oxidation of glycerol: Perspectives for high value chemicals. *Green Chem.* **2011**, *13*, 1960–1979. [CrossRef]
24. Bizot, P.M.; Bailey, B.R.; Hicks, P.D. Use of Tartronic Acid as an Oxygen Scavenger. Available online: <https://patentscope.wipo.int/search/en/detail.jsf?docId=WO1998016475> (accessed on 16 June 2020).
25. Pagliaro, M.; Rossi, M. The Future of Glycerol: New Usages for a Versatile Raw Material. Available online: <https://pubs.rsc.org/en/content/ebook/978-0-85404-124-4> (accessed on 16 June 2020).
26. Caselli, G.; Monatovanini, M.; Gandolfi, C.A.; Allegretti, M.; Fiorentino, S.; Pellegrini, L.; Melillo, G.; Bertini, R.; Sabbatini, W.; Anacardio, R.; et al. Tartronates: A new generation of drugs affecting bone metabolism. *J. Bone Miner. Res.* **1997**, *12*, 972–981. [CrossRef]
27. Carrettin, S.; McMorn, P.; Johnston, P.; Griffin, K.; Hutchings, G.J. Selective oxidation of glycerol to glyceric acid using a gold catalyst in aqueous sodium hydroxide. *Chem. Commun.* **2002**, 696–697. [CrossRef]
28. Porta, F.; Prati, L. Selective oxidation of glycerol to sodium glycerate with gold-on-carbon catalyst: An insight into reaction selectivity. *J. Catal.* **2004**, *224*, 397–403. [CrossRef]
29. Cai, J.; Ma, H.; Zhang, J.; Du, Z.; Huang, Y.; Gao, J.; Xu, J. Catalytic oxidation of glycerol to tartronic acid over Au/HY catalyst under mild conditions. *Chin. J. Catal.* **2014**, *35*, 1653–1660. [CrossRef]
30. Villa, A.; Veith, G.M.; Ferri, D.; Weidenkaff, A.; Perry, K.A.; Campisi, S.; Prati, L. NiO as a peculiar support for metal nanoparticles in polyols oxidation. *Catal. Sci. Technol.* **2013**, *3*, 394–399. [CrossRef]
31. Wang, D.; Villa, A.; Su, D.; Prati, L.; Schlogl, R. Carbon-supported gold nanocatalysts: Shape effect in the selective glycerol oxidation. *ChemCatChem* **2013**, *5*, 2717–2723. [CrossRef]

32. Sobczak, I.; Jagodzinska, K.; Ziolk, M. Glycerol oxidation on gold catalysts supported on group five metal oxides—A comparative study with other metal oxides and carbon based catalyst. *Catal. Today* **2010**, *158*, 121–129. [[CrossRef](#)]
33. Wolski, L. Factors affecting the activity and selectivity of niobia-based gold catalysts in liquid phase glycerol oxidation. *Catal. Today* **2020**, *354*, 36–43. [[CrossRef](#)]
34. Murthy, P.R.; Selvam, P. The enhanced catalytic performance and stability of ordered mesoporous carbon supported nano-gold with high structural integrity for glycerol oxidation. *Chem. Rec.* **2019**, *19*, 1913–1925. [[CrossRef](#)]
35. Zope, B.N.; Davis, S.E.; Davis, R.J. Influence of reaction conditions on diacid formation during Au-catalyzed oxidation of glycerol and hydroxymethylfurfural. *Top. Catal.* **2012**, *55*, 24–32. [[CrossRef](#)]
36. Pakrieva, E.; Ribeiro, A.P.C.; Kolobova, E.; Martins, L.M.D.R.S.; Carabineiro, S.A.C.; German, D.; Pichugina, D.; Jiang, C.; Pombeiro, A.J.L.; Bogdanchikova, N.; et al. Supported gold nanoparticles as catalysts in peroxidative and aerobic oxidation of 1-phenylethanol under mild conditions. *Nanomaterials* **2020**, *10*, 151. [[CrossRef](#)]
37. Pakrieva, E.; Kolobova, E.; Kotolevich, Y.; Pascual, L.; Carabineiro, S.A.C.; Kharlanov, A.N.; Pichugina, D.; Nikitina, N.; German, D.; Zepeda Partida, T.A.; et al. Effect of gold electronic state on the catalytic performance of nano gold catalysts in n-octanol oxidation. *Nanomaterials* **2020**, *10*, 880. [[CrossRef](#)]
38. Kolobova, E.; Maki-Arvela, P.; Pestryakov, A.; Pakrieva, E.; Pascual, L.; Smeds, A.; Rahkila, J.; Sandberg, T.; Peltonen, J.; Murzin, D.Y. Reductive amination of ketones with benzylamine over gold supported on different oxides. *Catal. Lett.* **2019**, *149*, 3432–3446. [[CrossRef](#)]
39. Kolobova, E.; Kotolevich, Y.; Pakrieva, E.G.; Mamontov, G.; Farias, M.H.; Bogdanchikova, N.; Pestryakov, A. Causes of activation and deactivation of modified nanogold catalysts during prolonged storage and redox treatments. *Molecules* **2016**, *21*, 486. [[CrossRef](#)]
40. Pakrieva, E.; Kolobova, E.; Mamontov, G.; Bogdanchikova, N.; Farias, M.H.; Pascual, L.; Cortés Corberán, V.; Martínez Gonzalez, S.; Carabineiro, S.A.C.; Pestryakov, A. Green oxidation of n-octanol on supported nanogold catalysts: Formation of gold active sites under combined effect of gold content, additive nature and redox pretreatment. *ChemCatChem* **2019**, *11*, 1615–1624. [[CrossRef](#)]
41. Kolobova, E.N.; Pakrieva, E.G.; Carabineiro, S.; Bogdanchikova, N.; Kharlanov, A.; Kazantsev, S.O.; Hemming, J.; Mäki-Arvela, P.; Pestryakov, A.N.; Murzin, D. Oxidation of a wood extractive betulin to biologically active oxo-derivatives using supported gold catalysts. *Green Chem.* **2019**, *21*, 3370–3382. [[CrossRef](#)]
42. Kolobova, E.; Mäki-Arvela, P.; Grigoreva, A.; Pakrieva, E.; Carabineiro, S.A.C.; Peltonen, J.; Kazantsev, S.; Bogdanchikova, N.; Pestryakov, A.; Murzin, D.Y. Catalytic oxidative transformation of betulin to its valuable oxo-derivatives over gold supported catalysts: Effect of support nature. *Cattod* **2020**. Accepted. [[CrossRef](#)]
43. Yang, J.; Guan, Y.; Verhoeven, T.; Santen, R.; Li, C.; Hensen, E.J.M. Basic metal carbonate supported gold nanoparticles: Enhanced performance in aerobic alcohol oxidation. *Green Chem.* **2009**, *11*, 322–325. [[CrossRef](#)]
44. Fang, W.; Chen, J.; Zhang, Q.; Deng, W.; Wang, Y. Hydrotalcite-supported gold catalyst for the oxidant-free dehydrogenation of benzyl alcohol: Studies on support and gold size effects. *Chem. Eur. J.* **2011**, *17*, 1247–1256. [[CrossRef](#)]
45. Ketchie, W.C.; Fang, Y.-L.; Wong, M.S.; Murayama, M.; Davis, R.J. Influence of gold particle size on the aqueous-phase oxidation of carbon monoxide and glycerol. *J. Catal.* **2007**, *250*, 94–101. [[CrossRef](#)]
46. Sankar, M.; Dimitratos, N.; Knight, D.W.; Carley, A.F.; Tiruvalam, R.; Kiely, C.J.; Thomas, D.; Hutchings, G.J. Oxidation of glycerol to glycolate by using supported gold and palladium nanoparticles. *ChemSusChem* **2009**, *2*, 1145–1151. [[CrossRef](#)]
47. Ketchie, W.C.; Murayama, M.; Davis, R.J. Selective oxidation of glycerol over carbon-supported AuPd catalysts. *J. Catal.* **2007**, *250*, 264–273. [[CrossRef](#)]

